

# Generator Turn-to-Turn Fault Protection Using a Stator-Rotor-Bound Differential Element

Bogdan Kasztenny, Normann Fischer, Héctor J. Altuve, and Douglas Taylor  
*Schweitzer Engineering Laboratories, Inc.*

Published in  
*Synchronous Generator Protection and Control: A Collection of  
Technical Papers Representing Modern Solutions, 2019*

Previously presented at  
RVP-AI 2019, July 2019,  
XIV Simposio Iberoamericano Sobre Proteccion de Sistemas  
Electricos de Potencia, February 2019,  
Southern African Power System Protection & Automation Conference, November 2017,  
and 8th Annual Protection, Automation and Control World Conference, June 2017

Original edition released April 2016

# Generator Turn-to-Turn Fault Protection Using a Stator-Rotor-Bound Differential Element

Bogdan Kasztenny, *Fellow, IEEE*, Normann Fischer, *Senior Member, IEEE*,  
Héctor J. Altuve, *Fellow, IEEE*, and Douglas Taylor, *Member, IEEE*

**Abstract**—Differential protection does not detect stator turn-to-turn faults in generators. Split-phase protection detects these faults but it is only applicable to generators with multiple stator circuits per phase. This paper proposes a new principle for generator turn-to-turn fault protection based on the ampere-turn balance between the stator negative-sequence current and the double-frequency component of the field current. The paper describes two protection elements using this principle: a stator-rotor current unbalance element that uses the current magnitudes and a stator-rotor current differential element that uses the current phasors. The paper derives the new methods, discusses their dependability, sensitivity, and security, and illustrates their operation with computer simulations and test results from a physical made-to-scale generator.

**Index Terms**—Generator protection, negative-sequence differential protection, generator stator faults, generator rotor faults, generator turn-to-turn faults.

## I. INTRODUCTION

FOR many years, the negative-sequence differential (87Q) principle has been applied to transmission line protection to detect high-resistance faults [1]. Recently, it has been applied to transformer protection, primarily for its sensitivity to turn-to-turn faults [2], [3], [4]. The 87Q principle follows Kirchhoff's current law in applications to transmission lines and the ampere-turn (AT) balance in applications to power transformers.

Stator differential protection—either per-phase or negative-sequence—does not detect turn-to-turn faults in generator stators because these faults do not upset Kirchhoff's current balance between the terminal- and neutral-side stator currents. Split-phase protection is the traditional solution for detecting turn-to-turn faults in large hydroelectric generators with split windings [5]. In other types of machines, the stator is often left unprotected against turn-to-turn faults.

This paper shows that applying the AT balance principle between the negative-sequence current ( $I_2$ ) in the stator and the double frequency component in the field current ( $I_F$ ) of the machine provides turn-to-turn fault protection for both the stator and rotor.

Based on this principle, the paper proposes a new protection element: the stator-rotor current unbalance (60SF) element, which balances the negative-sequence stator current magnitude with the properly ratio-matched magnitude of the double-frequency component in the field current.

The paper also describes a stator-rotor current differential (87SF) element using the machine stator and rotor current phasors. It shows how to perform the differential comparison of two currents despite them having different frequencies. The paper also explains how the differential element adapts for the change in rotor positions with respect to the stator as the output power of the machine changes.

The paper discusses the dependability, sensitivity, and security of the new elements and provides results from computer simulations and test results from a physical made-to-scale generator.

## II. STATOR-ROTOR-BOUND PROTECTION

With reference to Fig.1, we can think of a generator as a rotating transformer with an equivalent positive-sequence winding and current ( $I_1$ ), a negative-sequence winding and current, a field winding and current, and a damper winding, if present. The negative-sequence current in the stator creates a rotating magnetic field in the opposite direction of the rotor rotation (both the rotor and the magnetic field rotate at a speed corresponding to the power system frequency  $\omega$ ). As a result, the negative-sequence current induces a double-frequency ( $2\omega$ ) current in the field winding and other parts of the rotor, including the damper windings (if any) and the rotor core surface.

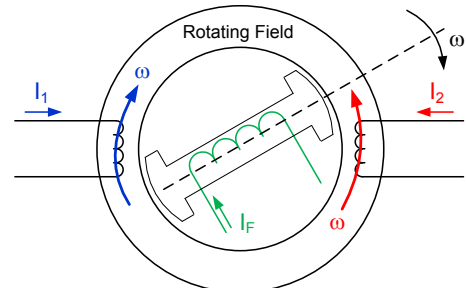


Fig. 1. The negative-sequence stator current induces double-frequency currents on the field and damper windings.

B. Kasztenny, N. Fischer, H. Altuve, and D. Taylor are with Schweitzer Engineering Laboratories, Inc., Pullman, WA 99163 USA (e-mail: papers@selinc.com).

In our analysis, we combine the double-frequency currents flowing in other parts of the rotor into one current, called the damper current, which flows in an equivalent damper winding. When looking at the machine from the stator side and considering the negative-sequence current, we can view the generator as a three-winding rotating transformer, having the stator winding fed with the negative-sequence current, the damper winding fed with a double-frequency current, and the field winding also fed with a double-frequency current, as depicted in Fig. 2a.

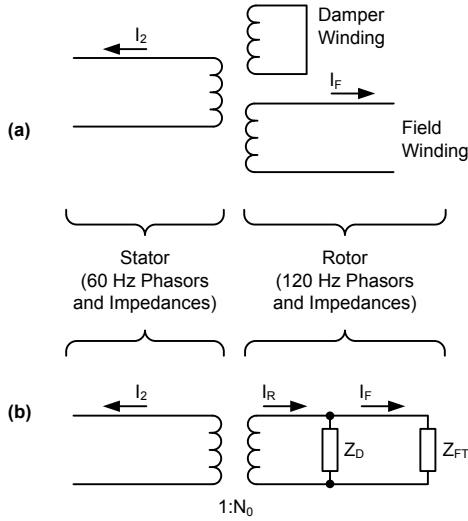


Fig. 2. An equivalent three-winding transformer relating the negative-sequence stator current and the double-frequency components of the field and damper windings brought to the same voltage base (a); two-winding representation with the field and damper windings brought to the same voltage base (b).

We can provide turn-to-turn fault protection for the stator and rotor of a machine by applying the AT balance to the equivalent three-winding transformer in Fig. 2a. We can measure the stator negative-sequence current and the double-frequency current component of the field. However, we are not able to measure the damper winding current. We can overcome this obstacle by examining Fig. 2b, in which we convert the damper and field impedances to the same voltage base and connect the two circuits in parallel to form a single equivalent winding. This way, we reduce the three-winding transformer to an equivalent two-winding transformer.

We assume the exciter does not generate any double-frequency voltage, and therefore, the field winding can be considered shorted with the total impedance of the field winding and the exciter circuit,  $Z_{FT}$ .  $Z_D$  is the damper winding leakage impedance. The  $Z_D$  and  $Z_{FT}$  impedances are double-frequency (120 Hz) impedances and are brought to the same voltage base.

Fig. 2b shows that we can provide turn-to-turn fault protection by applying the AT balance between the negative-sequence current ( $I_2$ ) in the stator and the total rotor current ( $I_R$ ). Again, we cannot measure the total rotor current.

However, as long as the damper impedance ( $Z_D$ ) and the total field circuit impedance ( $Z_{FT}$ ) are constant, we can calculate the total rotor current ( $I_R$ ) from the measured field current ( $I_F$ ):

$$I_R = I_F \cdot \left( 1 + \frac{Z_{FT}}{Z_D} \right) \quad (1)$$

The phasors and impedances in (1) are double-frequency (120 Hz) quantities.

Assuming the turn ratio of the equivalent two-winding transformer is  $N_0$ , the AT balance condition for any external unbalance in a healthy generator is:

$$I_2 = N_0 \cdot I_R = N_0 \cdot I_F \cdot \left( 1 + \frac{Z_{FT}}{Z_D} \right) \quad (2)$$

In other words, for any external unbalance, including faults, the ratio  $N_{SF}$  of the magnitudes of the negative-sequence stator current and the double-frequency field current for a healthy machine is:

$$N_{SF} = \left| \frac{I_2}{I_F} \right| = N_0 \cdot \left| 1 + \frac{Z_{FT}}{Z_D} \right| \quad (3)$$

A turn-to-turn fault in the rotor or stator will upset the AT balance conditions (2) and (3), which allows the detection of such faults.

In order to test this hypothesis, we simulated external faults and internal turn-to-turn faults in a sample 200 MW, 13.8 kV machine using the Real Time Digital Simulator (RTDS<sup>®</sup>) [6], [7].

Fig. 3 shows the terminal voltages and currents for an external phase-to-phase fault at the system side of the generator step-up transformer.

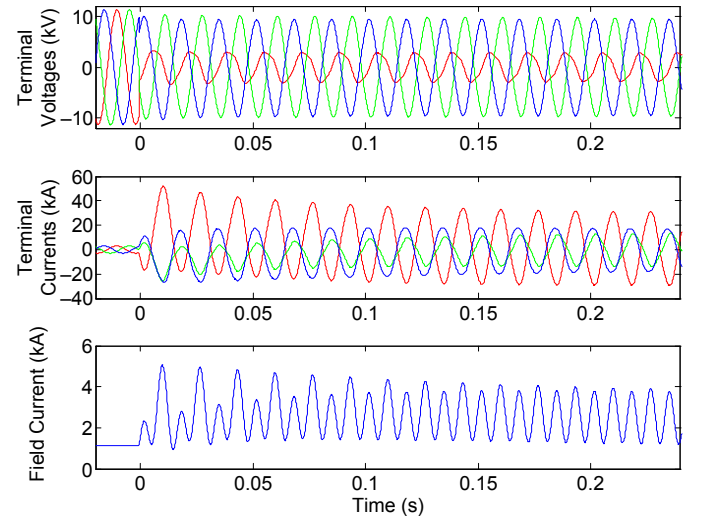


Fig. 3. External fault: terminal voltages and currents and field current.

Fig. 4 shows voltages and currents for a 5 percent turn-to-turn fault while the machine was loaded at 200 MW. A 5 percent turn-to-turn fault is the lowest percentage turn-to-turn fault that can be presently modeled in the RTDS [7].

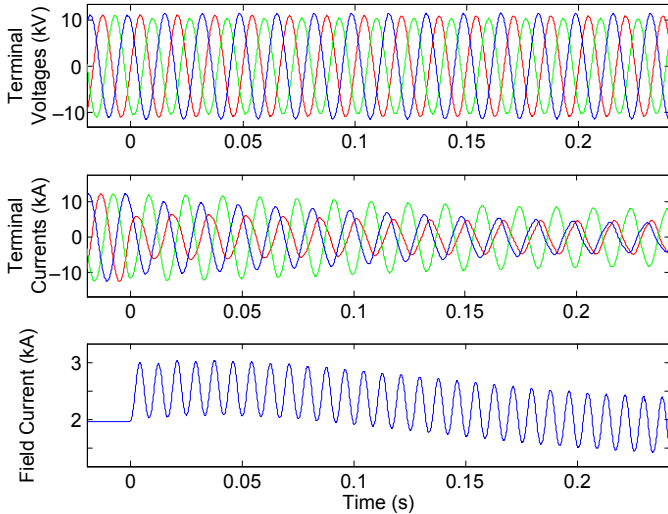


Fig. 4. Turn-to-turn fault: terminal voltages and currents and field current.

Fig. 5 shows the magnitudes of currents  $I_2$  and  $I_F$  and their ratio for the external fault case of Fig. 3. The  $I_2/I_F$  magnitude ratio settles at a value of approximately 13.4 for this external unbalance.

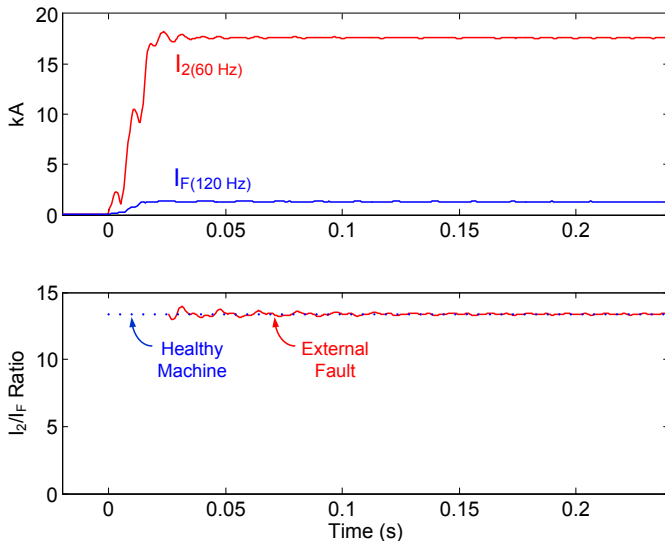


Fig. 5. External fault of Fig. 3: negative-sequence current magnitude (60 Hz), field current magnitude (120 Hz), and magnitude ratio.

The 13.4 ratio for this particular machine should apply for any external unbalance condition. We tested this premise by simulating a number of external phase-to-phase and single-phase-to-ground faults with the  $I_2$  magnitude varying between 175 A and about 17 kA. Fig. 6 shows these external faults as dots on the  $I_2$  versus  $I_F$  current magnitude plane. As we can see, all the external fault cases plot as a straight line with a slope of 13.4.

Having concluded that the  $I_2/I_F$  magnitude ratio holds constant for external faults, we now direct our attention to turn-to-turn faults. Fig. 7 shows the key signals for the simulated 5 percent turn-to-turn fault of Fig. 4. Note that for this fault, the  $I_2/I_F$  magnitude ratio is about 6 (compared with 13.4 for a healthy machine). In other words, instead of having an  $I_F$  magnitude of about  $3 \text{ kA}/13.4 = 220 \text{ A}$  for  $I_2 = 3 \text{ kA}$ , the

machine exhibits an  $I_F$  magnitude of about 500 A. Such a significant difference allows us to detect this turn-to-turn fault very reliably.

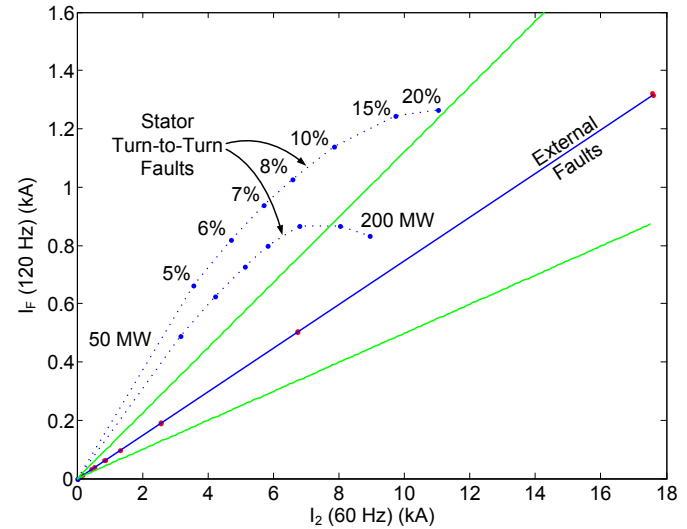


Fig. 6. Negative-sequence stator current magnitude versus double-frequency field current magnitude for external faults and turn-to-turn faults.

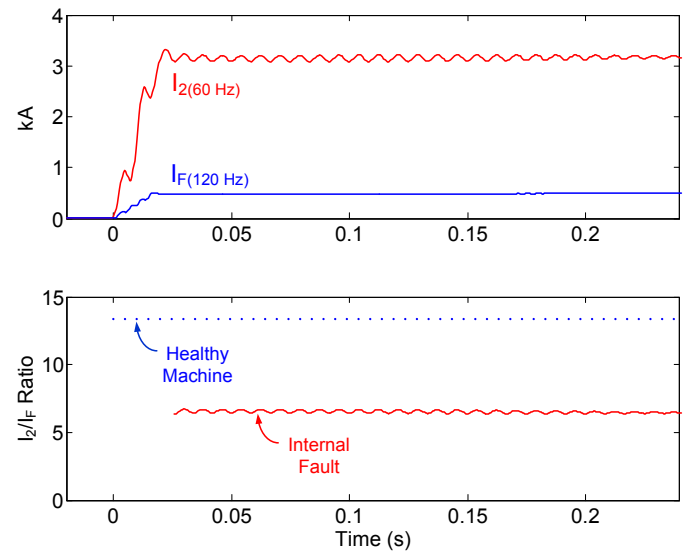


Fig. 7. Turn-to-turn fault of Fig. 4: negative-sequence current magnitude (60 Hz), field current magnitude (120 Hz), and magnitude ratio.

Fig. 6 shows the plot of a number of turn-to-turn faults on the  $I_2$  versus  $I_F$  current magnitude plane for generator loads of 50 MW and 200 MW. As we can see, these faults are located away from the straight line for external faults. The measured magnitude of  $I_F$  depends on the machine loading and is higher for a lightly loaded machine. Even for a fully loaded machine, the  $I_2/I_F$  magnitude ratio for turn-to-turn faults involving less than 10 percent of the turns differs by about 100 percent compared with the healthy machine. For faults involving 20 percent or more of the turns, the ratio is a less effective decision factor, especially for a heavily loaded machine, but these faults are very unlikely.

Note that the 5 percent turn-to-turn faults plot a considerable distance from the line of external faults. We

know that for turn-to-turn faults approaching 0 percent of shorted turns, there is no negative-sequence current in the stator or double-frequency current in the field winding. Therefore, we can extrapolate the dashed lines in Fig. 6 toward the origin of the plot. By doing so, we can see that the outlined principle will work well for turn-to-turn faults involving much less than 5 percent of the turns (the RTDS model we used is limited to 5 percent of the turns as the minimum turn-to-turn fault [7]). The physical model testing results described in Section V confirm this hypothesis.

### III. STATOR-ROTOR CURRENT UNBALANCE ELEMENT

Based on the principle derived above, we propose a new protection element: the stator-rotor current unbalance (60SF) element. As shown in Fig. 8, the relay measures the stator currents to calculate the negative-sequence stator current magnitude. It measures the field current (using a shunt, for example) to calculate the double-frequency field current magnitude.

The relay applies the effective transformation ratio ( $N_{SF}$ ) to match the magnitudes and checks if the two current magnitudes balance.

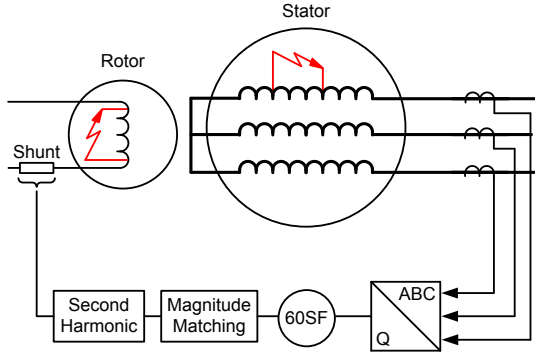


Fig. 8. The 60SF turn-to-turn fault protection element for synchronous generators.

A simple implementation of the 60SF element uses the following operating signal:

$$I_{OP} = \left| I_{2(60\text{ Hz})} - N_{SF} \cdot I_{F(120\text{ Hz})} \right| \quad (4)$$

and the following restraining signal:

$$I_{RST} = \left| I_{2(60\text{ Hz})} + N_{SF} \cdot I_{F(120\text{ Hz})} \right| \quad (5)$$

where the setting  $N_{SF}$  is the effective ratio between the two currents for a healthy machine.

Comparing the operating signal (4) with a percentage (a slope value) of the restraining signal (5) results in the operating characteristic shown by the green lines in Fig. 6 for a slope setting value of 20 percent. The restraining region is the area between the green lines, and the operating region is the area outside the green lines.

The currents involved in (4) and (5) are in primary amperes or properly matched secondary amperes. We calculate the  $I_{2(60\text{ Hz})}$  phasor using a filter tuned at the fundamental system frequency and extract the  $I_{F(120\text{ Hz})}$  phasor using a filter tuned at

double the system frequency. For accuracy, the two filters process frequency-tracked samples or use an equivalent method to ensure measurement accuracy should the frequency change.

In order to illustrate the operation of the 60SF element using (4) and (5), we simulated an external phase-to-phase fault, which evolved into a 5 percent turn-to-turn fault in our sample 200 MW, 13.8 kV machine loaded at 100 MW. Fig. 9 shows the terminal voltages and currents and the field current. Fig. 10 shows the  $I_2$  and  $I_F$  magnitudes and their ratio. The ratio remains at 13.4 during the external fault as expected and changes dramatically to about 6 when the turn-to-turn fault is simultaneously introduced 5 cycles into the external fault. Fig. 11 shows this case on the operating-restraining current plane per (4) and (5) with a slope setting of 20 percent. The trajectory first settles in the restraining region in response to the external fault and moves into the operating region once the turn-to-turn fault is introduced.

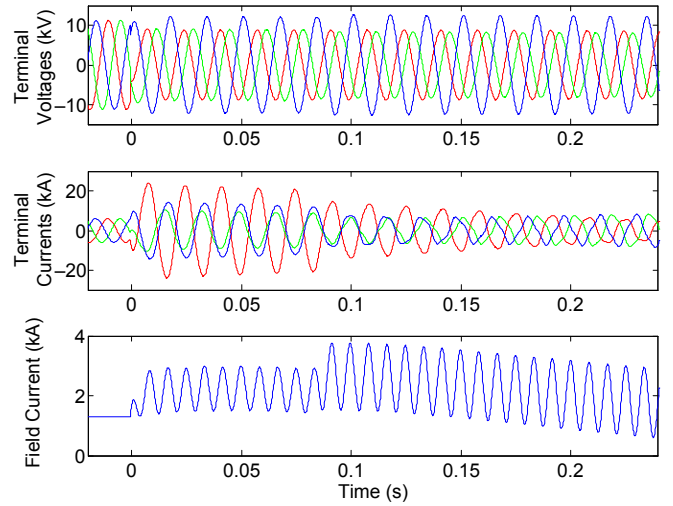


Fig. 9. Evolving external-to-internal fault: terminal voltages and currents and field current.

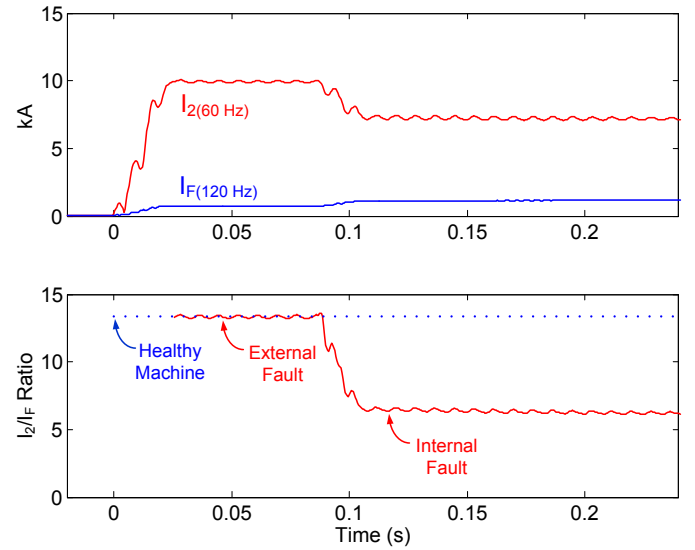


Fig. 10. Evolving external-to-internal fault: negative-sequence current magnitude (60 Hz), field current magnitude (120 Hz), and their magnitude ratio.

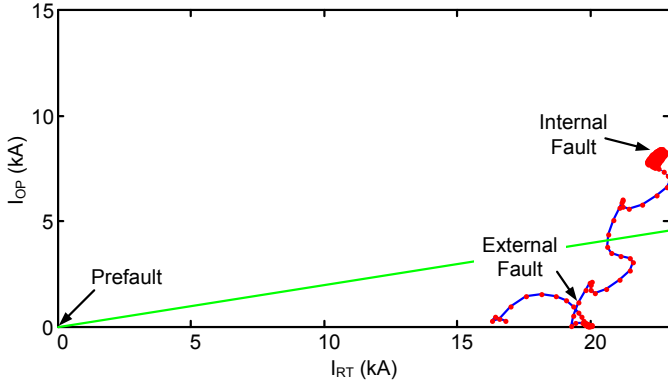


Fig. 11. Evolving external-to-internal fault: fault trajectory on the operating-restraining current plane per (4) and (5).

#### IV. STATOR-ROTOR CURRENT DIFFERENTIAL ELEMENT

So far, we have only used the magnitudes of the two currents involved in the AT balance between the rotor and stator of the machine. Can we develop a current differential element using the machine stator and rotor current phasors and gain more sensitivity as compared with using just the magnitudes? How much sensitivity can we gain?

We have to solve the following two challenges to establish a phasor-based current differential (87SF) element:

- First, the two compared currents are of different frequencies and their phasors rotate at different angular velocities (i.e., at the system frequency and double the system frequency).
- Second, the rotor changes positions with respect to the stator depending on the output power of the generators. Therefore, the phase shift between the two currents depends on the output power.

The first challenge can be solved by slowing down the field current double-frequency phasor by dividing it by a unity vector that rotates at the system frequency (demodulating with the system frequency). One simple implementation of this principle is to use the positive-sequence voltage phasor as follows:

$$I_{F(60\text{ Hz})} = I_{F(120\text{ Hz})} \cdot \frac{|V_1|}{V_1} \quad (6)$$

The advantages of using (6) are that we do not need to use the frequency explicitly and the calculation is correct even as the frequency changes slightly during faults.

With regard to the second challenge, our simulations show that to ensure proper phase relationships between the two compared currents for external unbalances, we need to shift the field current given by (6) by the following angle:

$$\Theta_C = \angle \left( \frac{E_{qPRE}}{V_{IPRE}} \right) + \frac{\pi}{2} \quad (7)$$

where  $V_{IPRE}$  is the predisturbance positive-sequence voltage (captured using simple disturbance detection) and:

$$E_{qPRE} = V_{IPRE} + jX_d \cdot I_{IPRE} \quad (8)$$

where  $I_{IPRE}$  is the predisturbance positive-sequence current and  $X_d$  is the generator direct axis reactance.

In other words, when using  $V_1$  for demodulation in (6), we need to rotate the current by the angle between  $V_1$  and  $E_d$ . This angle equals the angle between  $V_1$  and  $E_q$  plus 90 degrees per (7) and (8). We can further combine (7) and (8) and use:

$$\Theta_C = \angle \left( \frac{j \cdot V_{IPRE} - X_d \cdot I_{IPRE}}{V_{IPRE}} \right) \quad (9)$$

In order to be able to use (6) and (9), we need to use voltage signals in the 87SF element in addition to the current signals and we must capture the prefault values of the stator voltages and currents. We also need to know the generator direct axis reactance. These requirements make the 87SF element more advanced than the simpler 60SF element.

Fig. 12 shows the properly aligned currents for the evolving fault case of Fig. 9. As expected, the two currents are equal in magnitude and out of phase for the external fault. Once the internal turn-to-turn fault occurs 5 cycles into the external fault, the magnitudes no longer match and the phases shift, allowing for a more sensitive fault detection.

A simple implementation of the 87SF element uses the following differential signal:

$$I_{DIF} = \left| I_{2(60\text{ Hz})} + N_{SF} \cdot I_{F(60\text{ Hz})} \cdot 1 \angle -\Theta_C \right| \quad (10)$$

and the following restraining signal:

$$I_{RST} = \left| I_{2(60\text{ Hz})} - N_{SF} \cdot I_{F(60\text{ Hz})} \cdot 1 \angle -\Theta_C \right| \quad (11)$$

Comparing the operating and restraining signals (10) and (11) in a slope equation results in a typical percentage differential characteristic.

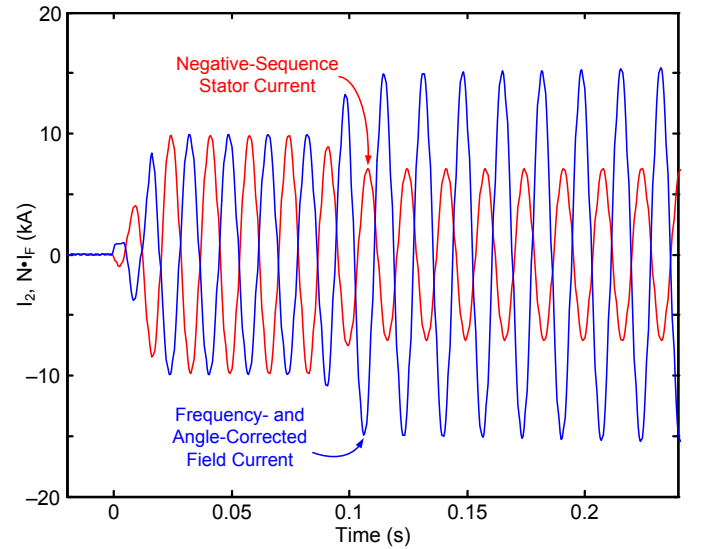


Fig. 12. Evolving external-to-internal fault: filtered negative-sequence stator current, and frequency-matched and angle-corrected field current.

Fig. 13 shows the block diagram of the 87SF element.

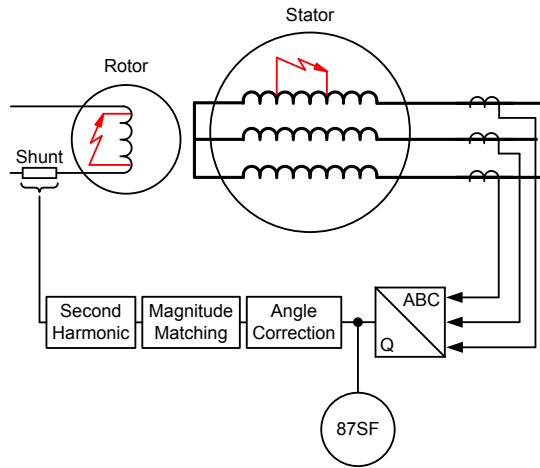


Fig. 13. The 87SF turn-to-turn fault protection element for synchronous generators.

Fig. 14 shows a trajectory of the evolving fault of Fig. 9 on the differential-restraining plane per (10) and (11) with a 20 percent slope setting. When the external fault occurs, the restraining signal increases to about 20 kA while the differential signal is very low. When the turn-to-turn fault occurs after 5 cycles, the differential signal increases to about 8 kA, yielding a reliable operation for this 5 percent turn-to-turn fault, despite the simultaneous external fault.

Comparing Fig. 11 (60SF) and Fig. 14 (87SF), we conclude that the two elements behave in a similar fashion, with the 87SF element having a slightly higher operating signal. This is because the phase angle between the two currents does not change much for this turn-to-turn fault (Fig. 12). If the phase angle changed more, the operating signal of the 87SF element would be even higher than that of the 60SF element. According to our simulations, differences in favor of the 87SF element are more visible for turn-to-turn faults on a heavily loaded machine.

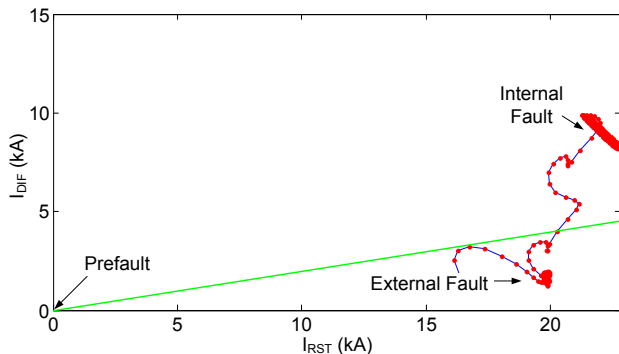


Fig. 14. Evolving external-to-internal fault: fault trajectory on the differential-restraining current plane per (10) and (11).

## V. PHYSICAL MODEL TESTING RESULTS

We tested the described protection elements using a three-phase 20 kVA, 220 V, three-pole laboratory generator driven by an induction motor (Fig. 15). The generator stator has 54 slots and two 100-turn windings per phase, with a 14/18 pitch. The windings have taps that allow applying 1, 2, 3, 5, and 10% turn-to-turn faults.



Fig. 15. Physical generator model.

Fig. 16 shows terminal voltages and currents, as well as the field current, for an external phase-to-phase fault at the laboratory generator terminals. Fig. 17 shows the magnitudes of currents  $I_2$  and  $I_F$  and their ratio for the external fault case of Fig. 16. The  $I_2/I_F$  magnitude ratio settles at about 40. We obtained similar results for external single-phase-to-ground faults.

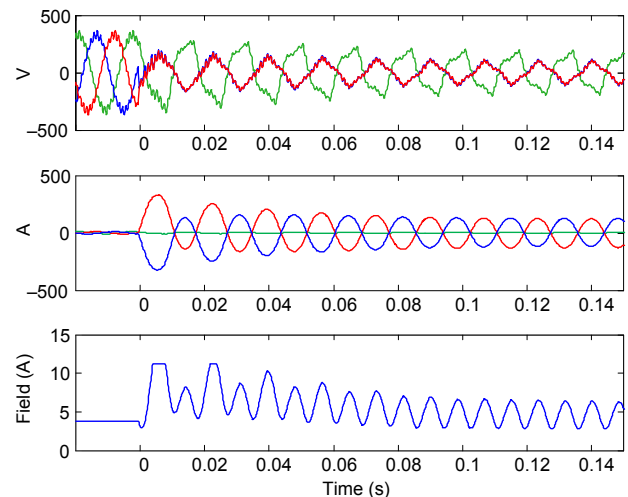


Fig. 16. External fault for the laboratory generator: terminal voltages and currents and field current.

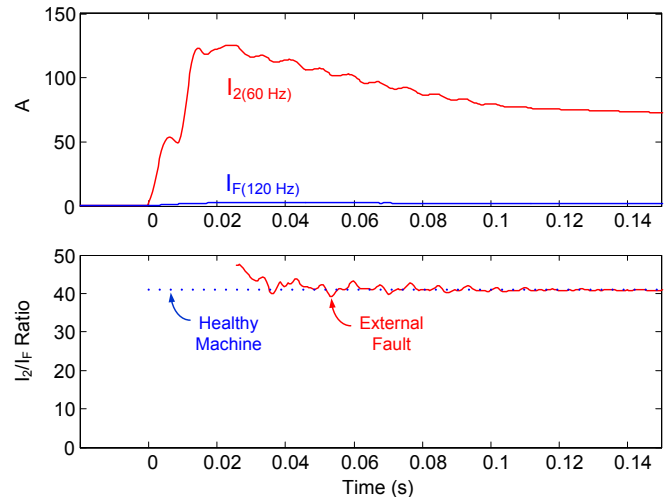


Fig. 17. External fault of Fig. 16: negative-sequence current magnitude (60 Hz), field current magnitude (120 Hz), and magnitude ratio.

We applied 1, 2, 3, 5, and 10 percent turn-to-turn faults at the laboratory generator stator. Fig. 18 shows a 3 percent turn-to-turn fault. Fig. 19 shows the signals for the 3 percent turn-to-turn fault of Fig. 18. For this fault, the  $I_2/I_F$  magnitude ratio

is about 50 (compared with 40 for a healthy machine). This difference allows us to detect this turn-to-turn fault very reliably. We obtained similar results for the other turn-to-turn faults, including the 1 percent fault, which is a single-turn fault at the 100-turn stator winding.

For internal turn-to-turn fault testing, we synchronized the laboratory generator to the laboratory system grid to provide an external power source that injects negative-sequence current to the generator stator windings. As mentioned earlier, an induction motor drives the synchronous generator. The problem with this setup is that as the output of the generator increases, the slip of the induction motor increases, which results in the synchronous speed of the generator decreasing (the generator frequency decreases from nominal). Hence, when the laboratory generator is synchronized to the local power system, it operates at the system frequency, which results in the synchronous generator functioning as a synchronous condenser and not delivering any active power to the power system. The generator stator current is extremely small and heavily distorted for this operating condition, as shown in Fig. 18.

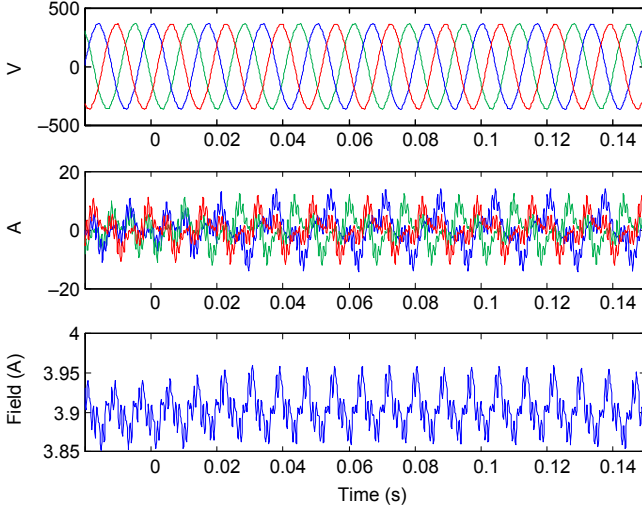


Fig. 18. Turn-to-turn fault at the laboratory generator stator: terminal voltages and currents and field current.

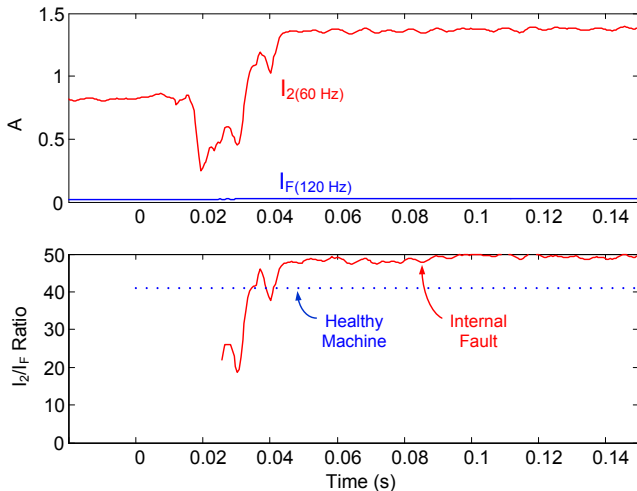


Fig. 19. Turn-to-turn fault of Fig. 18: negative-sequence current magnitude (60 Hz), field current magnitude (120 Hz), and magnitude ratio.

## VI. DISCUSSION OF 60SF AND 87SF ELEMENTS

In the previous sections, we introduced two novel elements for turn-to-turn fault protection of synchronous generators. We validated these elements with digital RTDS simulations and a physical generator model. Work is still needed to gain full confidence in the two protection elements.

At this time, we offer the following comments:

- Both the 60SF and 87SF elements are extensions of the 87Q element, because they balance the negative-sequence current in the stator against the resulting second-harmonic current in the field winding.
- The 60SF and 87SF elements are very sensitive and detect both stator and rotor turn-to-turn faults. Detection of rotor turn-to-turn faults requires an external current unbalance, such as an open phase or a fault, to create the negative-sequence signal, which in turn allows us to detect the fault.
- The 60SF and 87SF elements are based on the assumption that the ratio between the damper current and the field current is constant. This is true if the impedances of the damper and field circuits at double system frequency are constant. More research is needed to validate this assumption and develop methods to deal with any variability.
- The 60SF and 87SF elements are based on the assumption that the exciter does not produce any double-frequency voltage during normal operation. This is a justified assumption, because the double-frequency current in the field would induce a stator negative-sequence current and a damper current. However, more research is needed to validate this assumption for practical exciter designs.
- The 60SF element is simpler than the 87SF element because it does not require frequency and angle correction. The two elements behave in a similar fashion for turn-to-turn faults. However, the 87SF element is slightly more sensitive, especially for heavily loaded machines.
- The 60SF and 87SF elements need a slight time delay (1 to 2 cycles) to deal with transient differences between the measurements of the two compared currents. These transient differences are expected because the two measurements use different filters (60 Hz and 120 Hz).
- The 60SF and 87SF elements are susceptible to CT saturation errors for external faults and need proper external fault detection logic [3], [8], [9].

## VII. CONCLUSION

Negative-sequence differential elements detect turn-to-turn faults in transformers because they monitor the AT balance and respond to any event (including turn-to-turn faults) that upsets this balance. However, 87Q elements applied to generator stators do not monitor the AT balance and are therefore blind to turn-to-turn faults.

This paper derives and explains two novel protection elements for generator turn-to-turn fault protection: 60SF and 87SF. These elements are based on the AT balance between the fields created by the stator negative-sequence current and the rotor double-frequency current. The elements do not require the damper currents to be measured and therefore can be practically applied as long as the impedances of the field and damper windings are constant.

The RTDS simulations prove that the two elements are very sensitive and detect 5 percent turn-to-turn faults. The elements are secure for all types of external faults.

The test results from a physical generator model confirm the simulation results and show that the two elements can detect 1 percent turn-to-turn faults.

### VIII. REFERENCES

- [1] J. Roberts, D. Tziouvaras, G. Benmouyal, and H. J. Altuve, "The Effect of Multiprinciple Line Protection on Dependability and Security," proceedings of the 55th Annual Georgia Tech Protective Relaying Conference, Atlanta, GA, May 2001.
- [2] M. J. Thompson, H. Miller, and J. Burger, "AEP Experience With Protection of Three Delta/Hex Phase Angle Regulating Transformers," proceedings of the 60th Annual Conference for Protective Relay Engineers, College Station, TX, March 2007.
- [3] A. Guzmán, N. Fischer, and C. Labuschagne, "Improvements in Transformer Protection and Control," proceedings of the 62nd Annual Conference for Protective Relay Engineers, College Station, TX, March 2009.
- [4] Z. Gajić, I. Brnčić, B. Hillström, F. Mekić, and I. Ivanković, "Sensitive Turn-to-Turn Fault Protection for Power Transformers," proceedings of the 32nd Annual Western Protective Relay Conference, Spokane, WA, October 2005.
- [5] IEEE Standard C37.102, IEEE Guide for AC Generator Protection.
- [6] B. Kasztenny, N. Fischer, and H. J. Altuve, "Negative-Sequence Differential Protection—Principles, Sensitivity, and Security," proceedings of the 41st Annual Western Protective Relay Conference, Spokane, WA, October 2014.
- [7] A. B. Dehkordi, A. M. Gole, and T. L. Maguire, "Real Time Simulation of Internal Faults in Synchronous Machines," proceedings of the 7th International Conference on Power System Transients, Lyon, France, June 2007.
- [8] B. Kasztenny, G. Benmouyal, H. J. Altuve, and N. Fischer, "Tutorial on Operating Characteristics of Microprocessor-Based Multiterminal Line Current Differential Relays," proceedings of the 38th Annual Western Protective Relay Conference, Spokane, WA, October 2011.
- [9] H. J. Altuve, N. Fischer, G. Benmouyal, and D. Finney, "Sizing Current Transformers for Line Protection Applications," proceedings of the 66th Annual Conference for Protective Relay Engineers, College Station, TX, April 2013.

### IX. BIOGRAPHIES



**Bogdan Kasztenny** (M'1995, S'M'1998, F'2008) is the R&D director of technology at Schweitzer Engineering Laboratories, Inc. He has over 25 years of expertise in power system protection and control, including 10 years of academic career and 15 years of industrial experience, developing, promoting, and supporting many protection and control products.

Dr. Kasztenny is a Senior Fulbright Fellow, Canadian representative of the CIGRE Study Committee B5, registered professional engineer in the province of Ontario, and an adjunct professor at the University of Western Ontario. Since 2011, Dr. Kasztenny has served on the Western Protective Relay Conference Program Committee. Dr. Kasztenny has authored about 200 technical papers and holds 30 patents.



**Normann Fischer** (M'2009, S'M'2012) received a Higher Diploma in Technology, with honors, from Technikon Witwatersrand, Johannesburg, South Africa, in 1988; a BSEE, with honors, from the University of Cape Town in 1993; a MSEE from the University of Idaho in 2005; and a Ph.D. from the University of Idaho in 2014. He joined Eskom as a protection technician in 1984 and was a senior design engineer in the Eskom protection design department for three years. He then joined IST Energy as a senior design engineer in 1996. In 1999, Normann joined Schweitzer Engineering Laboratories, Inc., where he is currently a fellow engineer in the research and development division. He was a registered professional engineer in South Africa and a member of the South African Institute of Electrical Engineers. He is also a member of the ASEE.



**Héctor J. Altuve** (S'M'1995, F'2015) received his BSEE degree in 1969 from the Central University of Las Villas in Santa Clara, Cuba, and his Ph.D. in 1981 from Kiev Polytechnic Institute in Kiev, Ukraine. From 1969 until 1993, Dr. Altuve served on the faculty of the Electrical Engineering School at the Central University of Las Villas. From 1993 to 2000, he served as professor of the Graduate Doctoral Program in the Mechanical and Electrical Engineering School at the Autonomous University of Nuevo León in Monterrey, Mexico. In 1999 through 2000, he was the Schweitzer Visiting Professor in the Department of Electrical Engineering at Washington State University. Dr. Altuve joined Schweitzer Engineering Laboratories, Inc. (SEL) in January 2001, where he is currently a distinguished engineer and dean of SEL University. He has authored and coauthored more than 100 technical papers and several books and holds four patents. His main research interests are in power system protection, control, and monitoring.



**Douglas Taylor** (M'2010) received his BSEE and MSEE degrees from the University of Idaho in 2007 and 2009, respectively. Since 2009, he has worked at Schweitzer Engineering Laboratories, Inc. and currently is a lead research engineer in research and development. Mr. Taylor is a registered professional engineer in Washington. His main interests are power system protection and power systems analysis. He has authored several technical papers and holds one patent.